JOURNAL OF MATERIALS SCIENCE 27 (1992) 6335–6340

Pressureless sintering and related reaction phenomena of Al_2O_3-doped B_4C

CHAE HYUN LEE, CHONG HEE KIM
Department of Ceramic Science and Engineering, Korea Advanced Institute of Science and Technology, Taejon, 305-701, Korea

The effects of alumina on the densification of boron carbide and related reaction phenomena in alumina-doped B_4C were studied. Pressureless sintering was conducted at various temperatures for 15 min in a flowing Ar atmosphere. The addition of alumina improved the densification of boron carbide. Maximum density of 96% theoretical was obtained with the 3 wt% alumina-doped B_4C sintered at 2150 °C. Abnormal (or exaggerated) grain growth was observed in the specimen containing more than 4 wt% alumina. In the B_4C–Al_2O_3 reaction couples, good wetting of the liquid phase on the boron carbide grains was observed. X-ray diffraction and Auger electron spectra showed that the $AlB_{12}C_2$ phase was formed by the reaction between boron carbide and alumina. It is suggested that these phenomena promote the densification of boron carbide.

1. Introduction

Boron carbide is one of the most interesting non-oxide covalent solids. It has high melting point (congruent melting at about 2450 °C), high elastic modulus (450 GPa), extremely high hardness (the only substances harder than boron carbide are diamond and cubic boron nitride), low density, and chemical inertness [1]. It has therefore been employed for wear components such as sand blasting nozzles and die tips, and lightweight ceramic armour [2]. Boron carbide has also been used for reactor control rods in nuclear power engineering because of its high neutron absorption ability [3]. High thermoelectromotive force is another interesting character of boron carbide. In combination with graphite, it can be used for high temperature thermocouples [4].

Despite the advantages described above, sintering of boron carbide to a dense body is restricted by its highly covalent bonding and surface diffusion characteristics. So far, hot pressing of boron carbide at about 2100 °C or somewhat lower with sintering aids is the routine procedure to obtain dense bodies [5, 6]. However, hot pressing is limited by its well known disadvantages: high cost, directional variation of mechanical properties parallel and perpendicular to the hot pressing axis, and restriction to relatively simple shapes.

Many attempts have been made recently at pressureless sintering of boron carbide, but with only limited success. Kuzenkova *et al.* [7] reported that densities up to 95% of theoretical density were obtained at 2250 °C by sintering abrasive grade boron carbide powders with surface areas of $3.8\ m^2\,g^{-1}$. Also, Stibbs *et al.* [8] reported that specimens of low porosity were obtained using relatively large amount of additives such as 5–10 % Al, Mg or TiB_2. Recently, independent works [9, 10] showed that densities up to 97% could be obtained on sintering in argon at a temperature range of 2150–2250 °C.

As another category of sintering aid for pressureless sintering, Vasilos and Dutta [6] reported that above 1950 °C, alumina was found to be an effective densifying aid through complex liquid phase interactions. However, the detailed results were not specified.

In the present work, the effects of alumina on the sintering behaviour and microstructure of boron carbide were studied, and B_4C–Al_2O_3 reaction couples were made for the investigation of reaction phenomena between the two substances.

2. Experimental procedure

The commercially available boron carbide (Grade HS, H. C. Starck, Berlin, Germany) and alumina (AKP-50, Sumitomo Chem. Co., Japan) powders were used in the as-received state.

Boron carbide powder had an average particle size of ~ 0.9 μm. The powder contained ~ 1 wt % oxygen and 0.4 wt % nitrogen and minor metallic impurities. Total carbon content and boron-to-carbon ratio of boron carbide powder were 21 wt % and 3.9, respectively. Alumina powder had specified purity of 99.99%.

Boron carbide and alumina (up to 5 wt %) powders were mixed in a centrifugal mill (Pulverisette 6, Fritsch, Germany) for 30 min using a polypropylene bottle and alumina balls and then dried. The dried mixtures were screened to − 60 mesh and die pressed to form pellets (14 mm in diameter) followed by cold isostatic pressing at 150 MPa. After oven drying at 75 °C for 24 h, the green compacts had densities of ~ 60 % of theoretical.

The specimens were fired in a graphite resistance furnace to 2150 °C in flowing argon and the temperature was measured pyrometrically to $\pm 5\,^{\circ}\mathrm{C}$. The heating rate to the sintering temperature was $25\,^{\circ}\mathrm{C\,min^{-1}}$ and holding time was 15 min. For the reaction couple, sintered alumina (1400 °C, 2 h in air) was embedded in boron carbide powder and then die pressed. This type of specimen was heat treated under the same conditions as described above.

The sintered densities of specimens were measured by the water immersion method. Specimens were polished to 1 μm diamond paste and thermally etched for microstructural evaluations. Microstructures were observed by optical microscopy (Olympus, Japan) and scanning electron microscopy (SEM, ETEC Autoscan Co., Hayward, CA, USA).

X-ray diffraction (XRD) analysis with nickel-filtered $\mathrm{Cu}K_{\alpha}$ radiation was conducted to determine the reaction products in the reaction couple and Auger electron spectroscopy (PHI 610, Perkin-Elmer, USA) was used for qualitative elemental analysis.

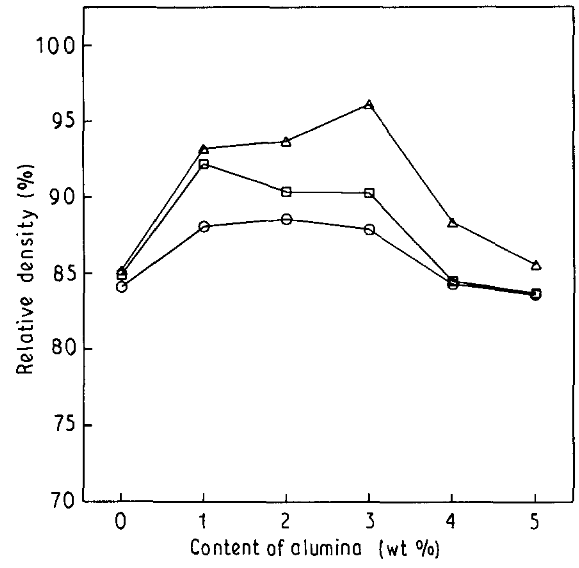

Figure 1 Sintered density changes as a function of alumina content at various sintering temperatures: △, 2150 °C; □, 2100 °C; ○, 2075 °C.

TABLE I Grain sizes of boron carbide ceramics as a function of alumina content

Alumina content (wt %)	0	1	3	5
Grain size[a] (μm)	3.63	5.35	7.07	8.92[b]

[a] Measured by linear intercept method.
[b] Abnormal grain growth was observed.

3. Results and discussion

3.1. Sintering behaviour and microstructure

Pressureless sintering of boron carbide was conducted with the addition of alumina up to 5 wt % to investigate the effects of alumina on the densification of boron carbide in a flowing argon atmosphere. Fig. 1 shows the results in terms of final densities after sintering at various temperatures for 15 min. When the sintering temperature was 2075 °C, the final densities could not exceed 87% of theoretical in all compositions. However, when the sintering temperature was raised to 2150 °C, the final densities increased to above 90%, with the composition range 1–3 wt % alumina additions. The best result (96% of theoretical) was obtained with a composition of 3 wt % alumina addition at a sintering temperature of 2150 °C.

Fig. 2a–c shows the microstructures of boron carbide with 0, 3 and 5 wt % alumina additions sintered at 2150 °C for 15 min. The equiaxed boron carbide grains are shown in the specimens containing up to 3 wt % alumina (Fig. 2a and b). In this composition range, the addition of alumina slightly increases the average grain size, as shown in Table I. However, as the addition of alumina exceeds 3 wt %, the microstructure shows large grains surrounded by small grains (Fig. 2c); exaggerated grain growth occurred. Exaggerated (or abnormal) grain growth in the sintering of boron carbide was described in recent reports [11, 12]. In these reports, the occurrence of abnormal grain growth was attributed to liquid phase. Its origins are eutectic and/or impurity melts in carbon-doped $\mathrm{B_4C}$ [11], and controlled liquid phase in the $\mathrm{B_4C{-}TiB_2{-}Fe}$ system [12]. In the present study, the sintering temperature of 2150 °C was higher than the melting point of alumina (about 2050 °C), so it seems that the abnormal grain growth shown in the composition of 5 wt % alumina content is due to the liquid phase.

On the other hand, the weight difference of specimens before and after sintering was measured. According to the data, weight loss occurred in all specimens and the amount of weight loss increased with increase of alumina content. From this result, it is supposed that some chemical reactions between boron carbide and alumina occurred during sintering, and some gas phase(s) might be contained in the reaction products. If so, there might be some decrease in density. The reaction between boron carbide and alumina will be discussed in the following section.

3.2. $\mathrm{B_4C{-}Al_2O_3}$ reaction couple

3.2.1. Microstructure

In this section, the reaction phenomena between boron carbide and alumina during sintering will be discussed. To this end, a reaction couple as shown in Fig. 3 was prepared. The optical micrograph in Fig. 3 shows the microstructure of the reaction couple after heat treatment at 2150 °C for 15 min. The white phase is boron carbide and the grey and dark phases are the liquid phase and pores, respectively.

Fig. 4a and b shows the magnified microstructures of the marked regions (designated as A and B, respectively) in the micrograph of Fig. 3. Fig. 4a shows the microstructure of the region at a distance from the interface region. Liquid phase can be observed both in grain boundaries (designated as B) and grain junctions (designated as J). The back-scattered electron image of this region (Fig. 4c) shows that the liquid phase contains a larger amount of heavy element (aluminium in

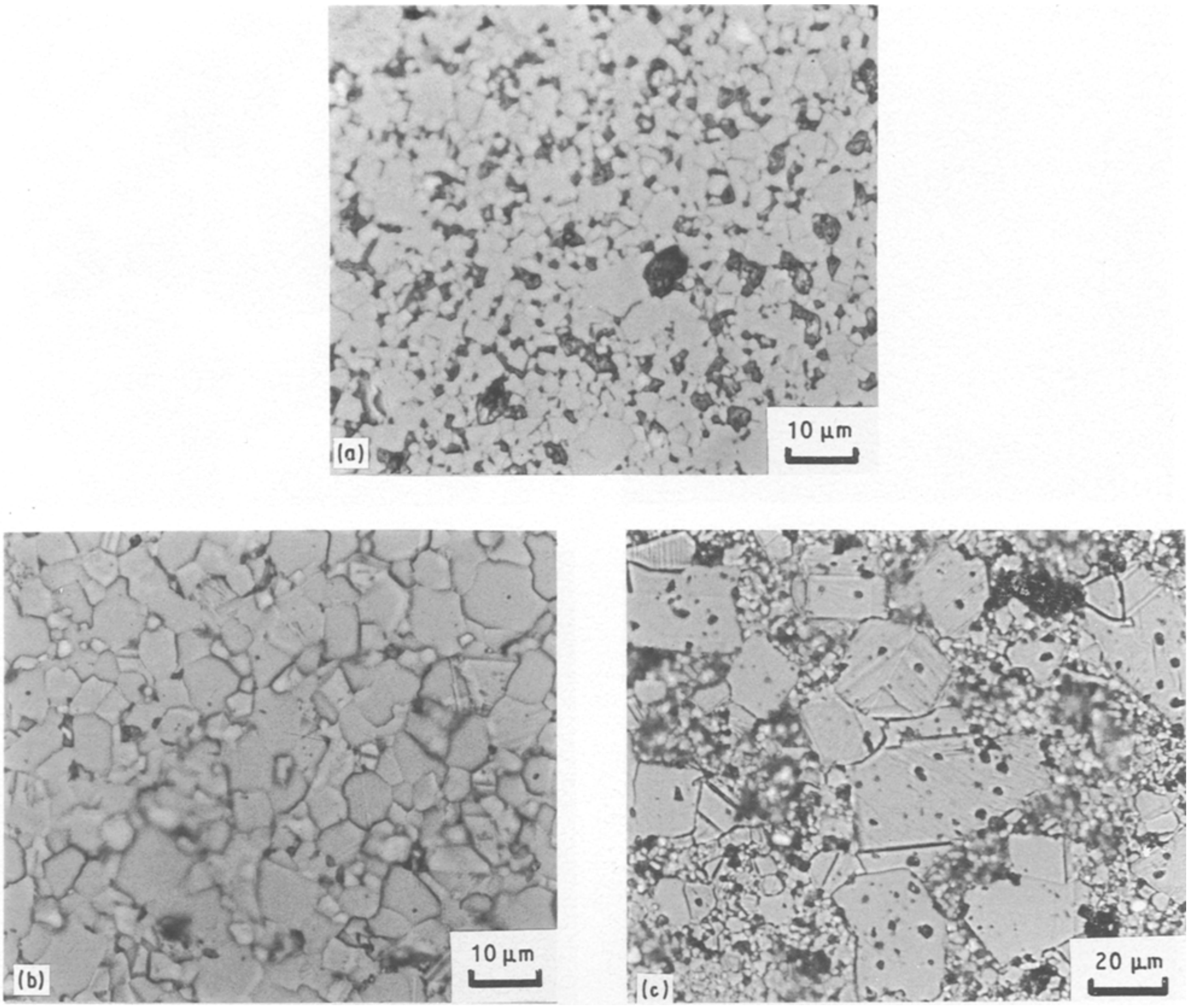

Figure 2 Optical micrographs of thermally etched specimens with alumina content of (a) 0 wt %, (b) 3 wt %, and (c) 5 wt % sintered at 2150 °C.

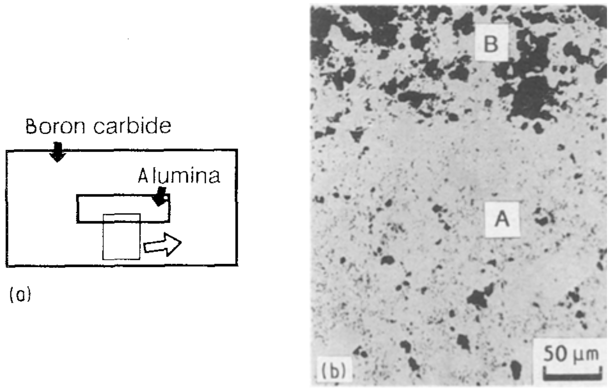

Figure 3 (a) Schematic and (b) low magnification micrograph of reaction couples. A and B indicate areas shown in greater detail in Fig. 4.

this case) than grains. An optical micrograph of the same region is shown in Fig. 5. Liquid phase is shown as the dark phase in the optical micrograph because the liquid phase has lower reflectivity than boron carbide grains. It can be observed that the liquid phase wets the grains well.

At the interface region of the sintering couple, the faceted grains 5–15 µm in size can be observed (Fig. 4b). Arrow marking in Fig. 4b seems to be liquid traces which existed during heat treatment. Fig. 4d is an X-ray scan of the Fig. 4a region for aluminium, which shows uniform distribution of aluminium throughout the micrograph. Thus it is considered that the faceted grains were grown into alumina melt and considered to be the aluminium-containing phase. It is reported that a non-wetting system can be transformed to a wetting system by taking advantage of chemical reactions [13]. Vasilos and Dutta [6] suggested the possibility of chemical reaction between boron carbide and alumina.

From the above results and aforementioned reports, two possibilities can be considered for good wetting of alumina melt on boron carbide, intrinsic behaviour or reaction-enhanced wetting. Further research is needed into this phenomenon.

3.2.2. Reaction products

XRD and Auger electron spectroscopy were conducted to identify the reaction products formed by the reaction between boron carbide and alumina.

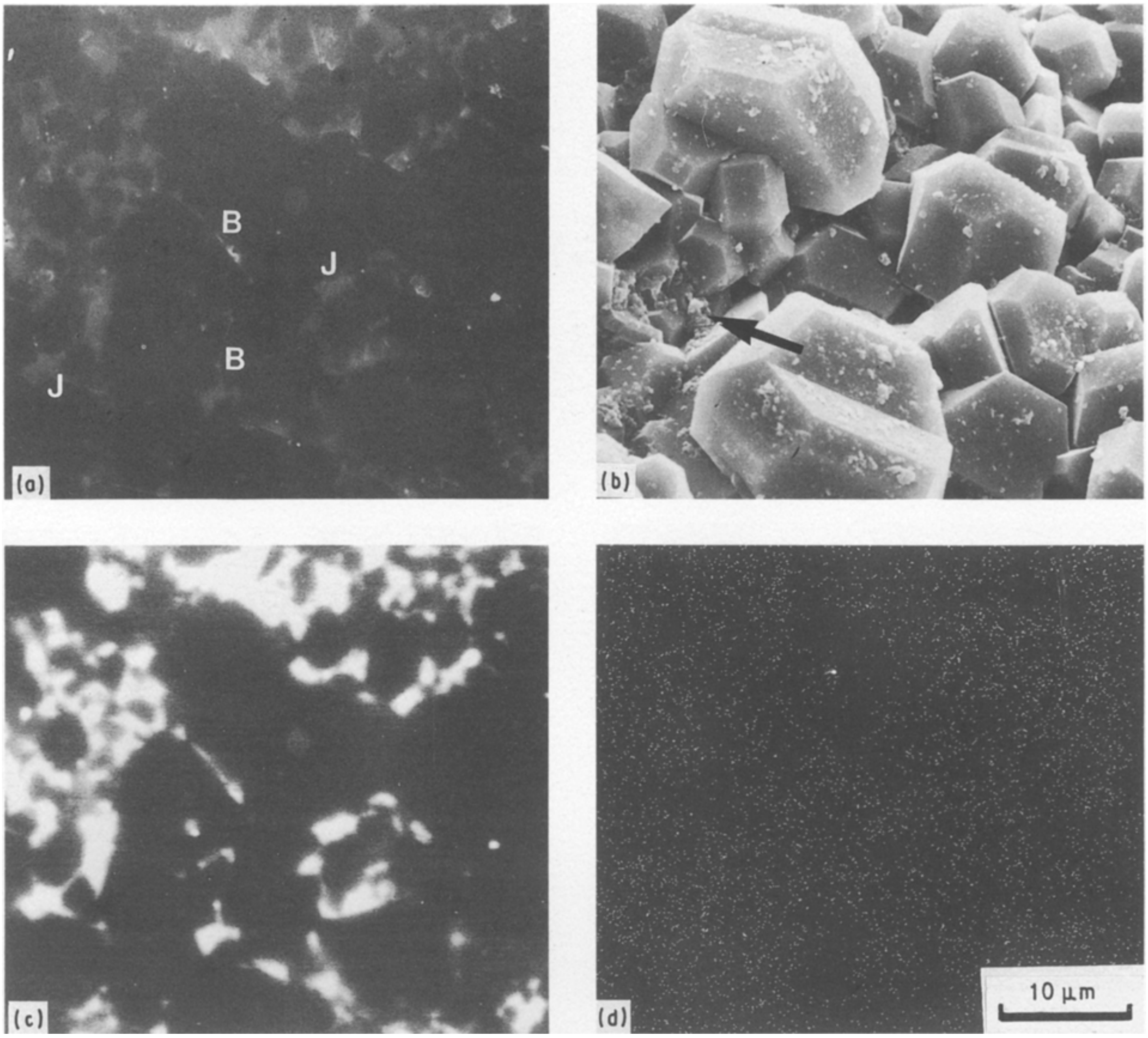

Figure 4 Microstructures of reaction couples; (a) scanning electron micrograph of polished section at bottom region; (b) scanning electron micrograph at interface region; (c) backscattered electron image of (a); and (d) X-ray scan of (b) for aluminium.

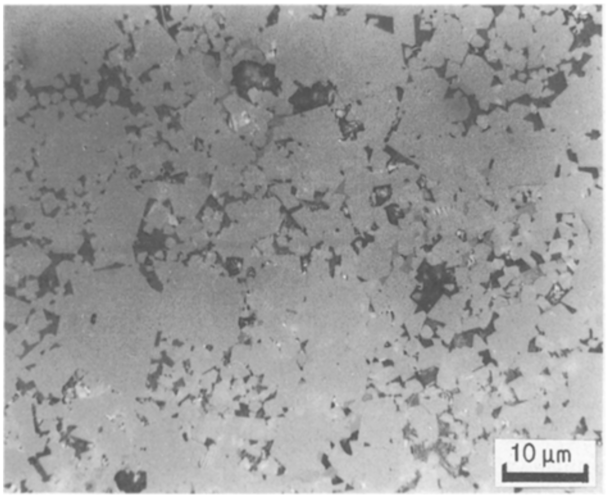

Figure 5 Optical micrograph showing good wetting of liquid phase on boron carbide grains.

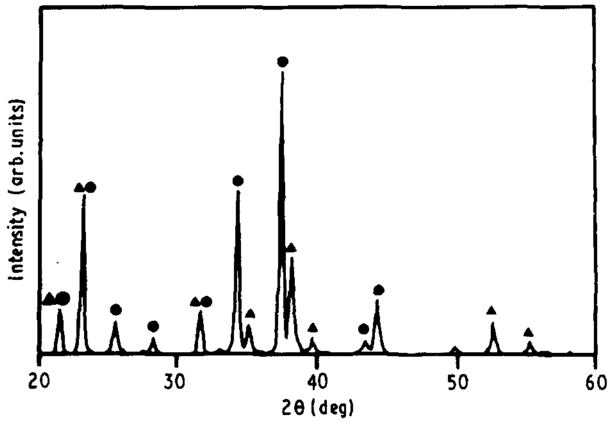

Figure 6 XRD pattern of reaction couple at interface region. ▲, B_4C; ●, $AlB_{12}C_2$.

Fig. 6 shows the XRD pattern of the reaction couple for the interface region. Main peaks were identified as boron carbide and $AlB_{12}C_2$ phase. The boron carbide phase is considered to be unreacted boron carbide and the $AlB_{12}C_2$ phase to be the reaction products in reaction couples. There are several binary and ternary phases in the B–C–Al system [14], and in B_4C–Al cermet systems [15, 16], reaction products detected by XRD include AlB_2, Al_4C_3, $AlB_{12}C_2$ and $AlB_{24}C_4$. However, only $AlB_{12}C_2$ phase was detected in this study. The relative amount of $AlB_{12}C_2$ phase increases with increase of distance from the bottom of the specimen, i.e. increase of reaction time.

Fig. 7 shows the Auger electron spectra for various regions in reaction couples. Boron, carbon, aluminium and oxygen peaks were detected in the liquid phase which existed in the bottom region of the reaction couple, i.e. short time from the beginning of reaction (Fig. 7a). No oxygen peak was detected and a small amount of aluminium was involved at the inside of grains (Fig. 7b), which existed in the same region as Fig. 4a. The Auger electron spectrum for the faceted grains at the interface region is shown in Fig. 7c. Boron, carbon and aluminium peaks were observed, but no oxygen peak was detected here. The content of aluminium atoms in this region was 6.8 at %; this value shows good accordance with the calculated value of 6.67 at % in the $AlB_{12}C_2$ phase, although the analysis conducted was qualitative. These results confirm the faceted phases to be $AlB_{12}C_2$ phase. Thus it is suggested that $AlB_{12}C_2$ phase was formed by reaction between boron carbide and alumina melt and good wetting of the melt enhanced by the reaction.

Possible reactions between boron carbide and alumina are as follows:

$$6B_4C + Al_2O_3 + C \rightarrow 2AlB_{12}C_2 + 3CO(g) \quad (1)$$

if a small amount of free carbon exists in boron carbide, and

$$AB_4C + BAl_2O_3 \rightarrow CAlB_{12}C_2 + DCO_x(g) \quad (2)$$

(where A, B, C and D are constants) when stoichiometric boron carbide was used. Both reactions result in weight losses due to the evolution of gas phase(s). In this study, chemical analysis of boron carbide powder revealed the existence of a small amount of free carbon. Thus the reaction that occurred in this study would be described by Equation 1.

Lange *et al.* [17] reported that when AlF_3 was added as a sintering aid for boron carbide, the $AlB_{12}C_2$ phase was formed by the following reaction

$$3B_4C + AlF_3 \rightarrow AlB_{12}C_2 + CF_3(g) \quad (3)$$

Further, they suggested that the $AlB_{12}C_2$ phase promotes the densification of boron carbide by lowering the diffusion energy barrier for densification.

Thus, from the above results, it is considered that densification of boron carbide with the addition of alumina was due to good wetting of alumina melt on boron carbide and lowering of the diffusion energy barrier for densification by the $AlB_{12}C_2$ phase. On the other hand, the evolution of gas phase(s) during sintering combined with abnormal grain growth could result in a decrease of final density, as mentioned in the previous section.

4. Conclusions

Sintering behaviour of boron carbide with addition of alumina and the reaction between boron carbide and alumina were studied. It is concluded that the addition of alumina up to 3 wt % promoted the densification of boron carbide and maximum density of 96% theoretical was obtained by sintering 3 wt % alumina-doped boron carbide at 2150 °C for 15 min. However, when the content of alumina exceeded 4 wt %, final densities decreased. This result was due to the abnormal (or exaggerated) grain growth and the weight loss during sintering. In the $B_4C-Al_2O_3$ reaction couples, good wetting of liquid phase on boron carbide grains was observed. XRD and Auger electron spectra showed that the $AlB_{12}C_2$ phase was formed by the reaction between boron carbide and alumina. It is suggested that these phenomena promoted the densification of boron carbide.

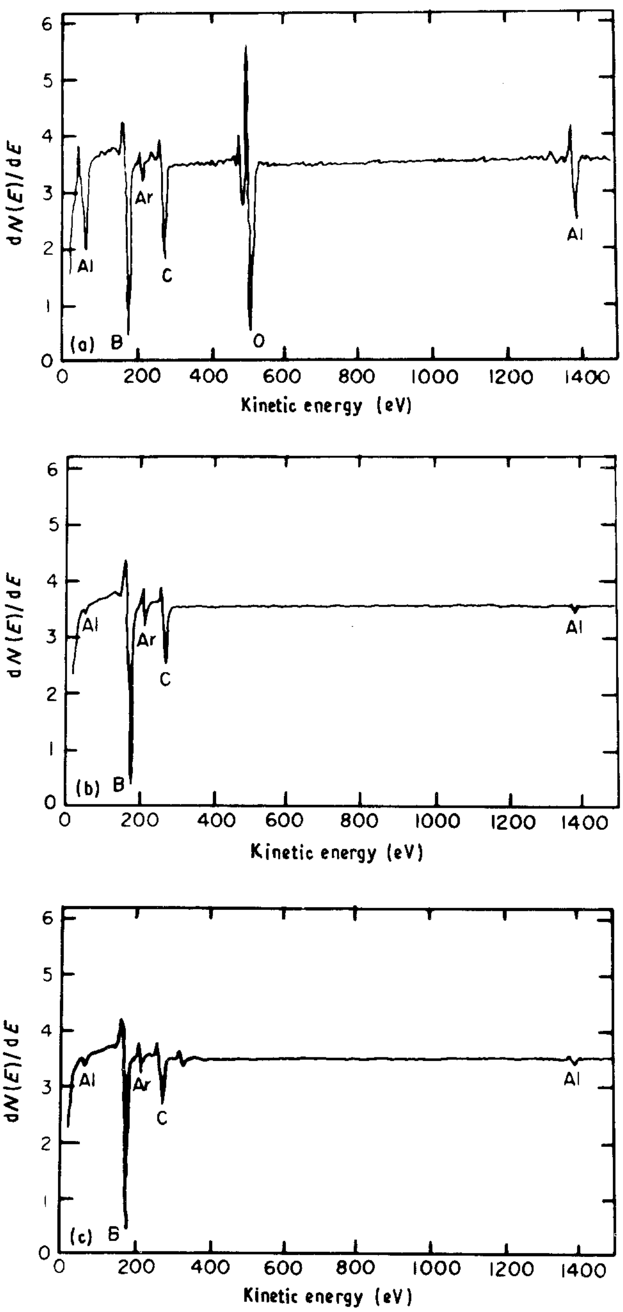

Figure 7 Auger electron spectra of reaction couples; (a) at liquid phase region of Fig. 4a; (b) at inside of grains of Fig. 4a; and (c) at interface region.

References

1. G. V. SAMSONOV and I. M. VINITSKII, "Handbook of Refractory Compounds", (IFI/Plenum, NY, 1980).

2. M. L. MILKINS, in "Boron and Refractory Borides", edited by V. I. Matkovich (Springer-Verlag, NY, 1977) p. 633.
3. K. REINMUTH, A. LIPP, H. KNOCH and K. A. SCHWETZ, *J. Nucl. Mat.* **124** (1984) 175.
4. Y. KANNO, *Yogyo-Kyokai-Shi* **94** (1986) 449.
5. R. ANGERS and M. BEAUVY, *Ceram. Int.* **10** (1983) 49.
6. T. VASILOS and S. K. DUTTA, *Amer. Ceram. Soc. Bull.* **53** (1973) 453.
7. M. A. KUZENKOVA, P. S. KISLYI, B. L. GRABCHUK and N. I. BODNARUK, *J. Less-Common Met.* **67** (1979) 217.
8. D. STIBBS, C. G. BROWN and R. THOMPSON, US Patent, 3 146 571 (1973).
9. K. A. SCHWETZ and W. GRELLNER, *J. Less-Common Met.* **82** (1981) 37.
10. S. L. DOLE and S. PROCHAZKA, *Ceram. Eng. Sci. Proc.* **6** (1985) 1151.
11. S. PROCHAZKA, S. L. DOLE and C. I. HEJNA, *J. Amer. Ceram. Soc.* **68** (1985) C-235.
12. D. K. KIM and C. H. KIM, *Adv. Ceram. Mat.* **3** (1988) 52.
13. I. A. AKSAY, C. E. HOGE and J. A. PASK, *J. Phys. Chem.* **78** (1974) 1178.
14. D. C. HALVERSON, A. J. PYZIK and I. A. AKSAY, *Ceram. Eng. Sci. Proc.* **6** (1985) 736.
15. D. C. HALVERSON, A. J. PYZIK, I. A. AKSAY, and W. E. SNOWDEN, *J. Amer. Ceram. Soc.* **72** (1989) 775.
16. A. J. PYZIK, I. A. AKSAY and M. SARIKAYA, in "Ceramic Microstructures '86 Role of Interface", edited by J. A. Pask and A. G. Evans (Plenum, New York, 1986) p. 45.
17. R. G. LANGE, Z. A. MUNIR and J. B. HOLT, in "Sintering Processes", edited by G. C. Kuczynski (Plenum, New York, 1979) p. 311.

Received 13 June
and accepted 31 October 1991